

Ytterbium-doped-garnet crystal waveguide lasers grown by pulsed laser deposition

STEPHEN J. BEECHER,^{*} JAMES A. GRANT-JACOB, PING HUA, JAKE J. PRENTICE, ROBERT W. EASON, DAVID P. SHEPHERD, AND JACOB I. MACKENZIE

Optoelectronics Research Centre, University of Southampton, Southampton, SO17 1BJ, UK

**S.J.Beecher@soton.ac.uk*

Abstract: The growth of a range of crystal garnets by pulsed laser deposition is presented. As a result of optimization of the fabrication process, films can now be grown with optical quality approaching that of bulk material. To demonstrate this, we present laser performance from a Yb:YAG film with 70% slope efficiency and >16 W of output power. In addition, we present the first pulsed laser deposition of laser quality Yb:GGG and Yb:YGG. Watt-level laser performance is achieved for these two gallium garnets and routes to further performance improvements and potential applications of these films are discussed.

Published by The Optical Society under the terms of the [Creative Commons Attribution 4.0 License](https://creativecommons.org/licenses/by/4.0/). Further distribution of this work must maintain attribution to the author(s) and the published article's title, journal citation, and DOI.

OCIS codes: (310.0310) Thin films; (220.4610) Optical fabrication; (230.7390) Waveguides, planar; (130.0130) Integrated optics; (140.3380) Laser materials; (140.5680) Rare earth and transition metal solid-state lasers.

References and links

1. C. L. Bonner, A. A. Anderson, R. W. Eason, D. P. Shepherd, D. S. Gill, C. Grivas, and N. Vainos, "Performance of a low-loss pulsed-laser-deposited Nd:Gd₃Ga₅O₁₂ waveguide laser at 1.06 and 0.94 μm," *Opt. Lett.* **22**(13), 988–990 (1997).
2. J. I. Mackenzie, "Dielectric solid-state planar waveguide lasers: a review," *IEEE J. Sel. Top. Quantum Electron.* **13**(3), 626–637 (2007).
3. K. A. Sloyan, T. C. May-Smith, M. Zervas, R. W. Eason, S. Huband, D. Walker, and P. A. Thomas, "Growth of crystalline garnet mixed films, superlattices and multilayers for optical applications via shuttered Combinatorial Pulsed Laser Deposition," *Opt. Express* **18**(24), 24679–24687 (2010).
4. R. Gazia, T. C. May-Smith, and R. W. Eason, "Growth of a hybrid garnet crystal multilayer structure by combinatorial pulsed laser deposition," *J. Cryst. Growth* **310**(16), 3848–3853 (2008).
5. S. H. Waeselmann, S. Heinrich, C. Kraenkel, and G. Huber, "Lasing of Nd³⁺ in sapphire," *Laser Photonics Rev.* **10**(3), 510–516 (2016).
6. R. Kumaran, S. E. Webster, S. Penson, W. Li, T. Tiedje, P. Wei, and F. Schiettekatte, "Epitaxial neodymium-doped sapphire films, a new active medium for waveguide lasers," *Opt. Lett.* **34**(21), 3358–3360 (2009).
7. T. L. Parsonage, S. J. Beecher, A. Choudhary, J. A. Grant-Jacob, P. Hua, J. I. Mackenzie, D. P. Shepherd, and R. W. Eason, "Pulsed laser deposited diode-pumped 7.4 W Yb:Lu₂O₃ planar waveguide laser," *Opt. Express* **23**(25), 31691–31697 (2015).
8. J. A. Grant-Jacob, S. J. Beecher, T. L. Parsonage, P. Hua, J. I. Mackenzie, D. P. Shepherd, and R. W. Eason, "An 11.5 W Yb:YAG planar waveguide laser fabricated via pulsed laser deposition," *Opt. Mater. Express* **6**(1), 91–96 (2016).
9. H. Kühn, S. T. Fredrich-Thornton, C. Kränkel, R. Peters, and K. Petermann, "Model for the calculation of radiation trapping and description of the pinhole method," *Opt. Lett.* **32**(13), 1908–1910 (2007).
10. M. J. Belovolov, E. M. Dianov, M. I. Timoschekhin, L. V. Barashov, A. M. Belovolov, M. A. Ivanov, N. P. Morosov, A. M. Prokhorov, and K. M. Timoschekhin, "Room temperature CW Yb:GGG laser operation at 1.038 μm," in *Proceedings of European Meeting of Lasers and Electro-Optics (CLEO/Europe, 1996)*, p43, paper CML5.
11. S. Chénais, F. Druon, F. Balembois, P. Georges, A. Brenier, and G. Boulon, "Diode-pumped Yb:GGG laser: comparison with Yb:YAG," *Opt. Mater.* **22**(2), 99–106 (2003).
12. H. Yu, K. Wu, B. Yao, H. Zhang, Z. Wang, J. Wang, Y. Zhang, Z. Wei, Z. Zhang, X. Zhang, and M. Jiang, "Growth and Characteristics of Yb-doped Y₃Ga₅O₁₂ Laser Crystal," *IEEE J. Quantum Electron.* **46**(12), 1689–1695 (2010).
13. W. Han, K. Wu, X. Tian, L. Xia, H. Zhang, and J. Liu, "Laser performance of ytterbium-doped gallium garnets: Yb:Re₃Ga₅O₁₂ (Re = Y, Gd, Lu)," *Opt. Mater. Express* **3**(7), 920–927 (2013).

14. J. M. Serres, V. Jambunathan, P. Loiko, X. Mateos, H. Yu, H. Zhang, J. Liu, A. Lucianetti, T. Mocek, K. Yumachev, U. Griebner, V. Petrov, M. Aguiló, and F. Diaz, "Microchip laser operation of Yb-doped gallium garnets," *Opt. Mater. Express* **6**(1), 46–57 (2016).
15. W. F. Krupke, "Ytterbium solid-state lasers - the first decade," *IEEE J. Sel. Top. Quantum Electron.* **6**(6), 1287–1296 (2000).
16. J. I. Mackenzie, J. W. Szela, S. J. Beecher, T. L. Parsonage, R. W. Eason, and D. P. Shepherd, "Crystal planar waveguides, a power scaling architecture for low-gain transitions," *IEEE J. Sel. Top. Quantum Electron.* **21**(1), 1601610 (2015).
17. S. J. Beecher, T. L. Parsonage, J. I. Mackenzie, K. A. Sloyan, J. A. Grant-Jacob, and R. W. Eason, "Diode-end-pumped 1.2 W Yb:Y₂O₃ planar waveguide laser," *Opt. Express* **22**(18), 22056–22061 (2014).

1. Introduction

Pulsed laser deposition (PLD) of thin layers of laser-active crystals has been of significant research interest since the mid 1990's [1], but until recently the waveguide laser performance obtained with these films has been relatively poor in comparison with similar waveguide devices made by other means [2]. The promise of this crystal growth technique lies in its ability to engineer the thickness of each layer with atomic-level precision and via a graded approach at significant growth rates, with ~20 μm per hour realized in our system for some garnet crystals. Additionally, due to the additive manner of the deposition, composite materials can be grown relatively simply through sequentially alternating the target material [3], or even enabling grading of the film properties, such as refractive index or dopant concentration, by tailoring the ablation rate between multiple targets [4]. This level of control for the refractive index profile and dopant distribution are beyond what can be achieved for other laser crystal fabrication methods. Historically, however, the optical quality of the films has been worse than that of bulk crystals limiting this technique to a research-only interest.

In the last year two major developments in the field of PLD have occurred. The first was the demonstration of lasing in Nd:sapphire, grown by PLD [5]. The interesting spectroscopy of this doped crystal had been known for some time [6], but no laser performance had been reported. Few growth methods are capable of producing this nonequilibrium phase and we assume that the initial reports for this material, grown by molecular beam epitaxy, had losses outweighing the achievable gain and preventing threshold from being reached. However, with the optimized PLD material, laser action was achieved with 137 mW of output power.

The second major development in PLD-grown laser material has been the improvement of film quality for the more established ytterbium-doped cubic oxide crystals, including both Yb:Lu₂O₃ and Yb:YAG. For an Yb:Lu₂O₃ film, over 7 W of output power was achieved at a slope efficiency of 38% [7], demonstrating the first efficient multi-Watt laser performance from PLD-grown material. This report was followed by an 11.5 W laser with a 48% slope efficiency based on PLD-grown Yb:YAG [8]. Since that report, further optimization of the crystal quality of the PLD-grown Yb:YAG has occurred; and here, we report on our improvements leading to a laser with a 70% slope efficiency. In addition, we also report on the early development of films of the ytterbium doped gallium garnet crystals Yb:GGG and Yb:YGG. Watt-class lasers have been produced from both of these materials and their spectroscopy is evaluated for comparison with the more established laser material Yb:YAG. It is our belief that with further optimization of growth conditions the performance from other garnet crystals can reach that of PLD-grown Yb:YAG. Furthermore, as some of these material, e.g. YGG or GGG have a significantly higher refractive index than the growth substrate, YAG, it is envisaged that we will be able to fabricate high numerical aperture waveguides (NA ~0.57 and 0.7, respectively). With additional engineering of these high quality crystals it will be possible to make "double-clad" structures that allow for efficient pumping with diode stacks, akin to the developments in high-power fiber lasers.

2. Crystal growth

The Yb:garnet films were grown from >99.9% purity source material of constituent oxides pressed and sintered into 50-mm-diameter disks, with a density exceeding 85% of that of bulk

single crystals. The targets were loaded into a custom-made rotary stage providing epitrochoidal movement, then ablated by a KrF excimer laser operating at 248 nm, providing uniform ablation of ~70% of the target area. Each growth was performed onto one 10 mm × 10 mm face of a 10 mm × 10 mm × 1 mm <100>-YAG substrate, which was heated from the opposing 10 mm × 10 mm face with a spatially homogenized 10.6 μm CO₂ laser. The target, rotary assembly and substrate are housed in a vacuum chamber, evacuated to 6 × 10⁻⁴ mbar and then backfilled to 2 × 10⁻² mbar with oxygen prior to growth. Laser access for the excimer beam for target ablation and the CO₂ beam for substrate heating occurred through anti-reflection (AR) coated windows. For the present work Yb:YAG, Yb:YGG and Yb:GGG were grown using a CO₂ laser power of 26.5 W, 17.5 W and 12.5 W and ablation fluence of 1.05 J/cm², 1.05 J/cm² and 1.25 J/cm² respectively, in all cases the ablation laser was operated at 20 Hz. Further details of correlations between growth parameters and material properties will be the subject of a future paper. Following deposition, two opposing end facets were lapped and polished plane-parallel resulting in ~8 mm waveguide lengths. The waveguides reported here are formed of a single layer of PLD material with a thickness of between 10 and 12 μm.

3. Gain media

To characterize the properties of the dopant ion within the PLD-grown crystal, the 10 mm × 10 mm face of the sample was excited with a ~960 nm diode laser focused to an irradiance significantly lower than the saturation value. Typically irradiances of <1 kW/cm² were used. The fluorescence is captured by a lens and focused onto a fast photodiode with pump light removed using a 1000 nm longpass filter. The measured lifetime of 950 μs for PLD-grown Yb:YAG agrees well with literature values for bulk crystals measured in such a way as to remove the effect of radiation trapping (e.g. the pinhole method [9]). For the gallium garnets, discrepancy exists within the literature as to the correct values of the lifetimes, for example for Yb:GGG, Belovolov *et al.* [10], report the lifetime as 0.8 ms in the first report of laser action in this material, but due to the brevity of the report make no mention of measurement technique. Chénais *et al.* [11], state that they measured the lifetime to be 1.56 ms, but believe radiation trapping to have corrupted their result and so they rely on the value of Belovolov, for evaluation of their cross sections. Other papers have referenced the Chénais paper choosing either the 0.8 or 1.56 ms value [12,13]. For YGG, Yu *et al.* [12] measure the lifetime to be 1.78 ms for a 10 at.% doped sample but do not, to the best of our knowledge, attempt to limit the contribution of radiation trapping. Han *et al.* quotes this result for the Yb:YGG lifetime [13], and Serres then references the Han paper, but quotes the lifetime as 1.1 ms [14]. Based on these issues, with previous data for these crystals, we believe our measured lifetimes of 985 μs for Yb:YGG and 1270 μs for Yb:GGG, taken in a geometry that minimizes radiation trapping, to be the most reliable currently available.

After measuring fluorescence lifetimes, pump light was launched into one of the waveguide facets and a multimode optical fiber (62.5 μm core, 0.22 NA) was positioned above the sample, capturing fluorescence and transmitting it to an optical spectrum analyzer. This collection geometry restricts the signal to photons emitted at angles outside of the waveguide numerical aperture, effectively avoiding any reshaping of the measured fluorescence spectrum by the spectrally dependent reabsorption of the material (the mean photon path through doped material is ~5 μm and the typical peak absorption lengths for these materials are 1 mm). The captured fluorescence spectra and measured fluorescence lifetimes were then used to calculate the emission cross section for the ion using the Fuchbauer-Landenburg equation. From these data and using literature values for the Stark levels of the crystals [12, 15], the absorption cross sections were estimated using the reciprocity method. It should be noted that Stark levels for Yb:YGG were used for the reciprocity method for both Yb:YGG and Yb:GGG due to the strong similarities in their emission spectra. This could lead to up to 10% error levels in the absorption cross sections for Yb:GGG. However, our calculated absorption cross section values appear to be consistent with the data taken by

Chénaïs *et al.* [11]. Some key spectroscopic parameters for the grown films are given in Table 1, and the emission and absorption cross sections are shown in Fig. 1. It can be seen that for most applications the spectroscopic properties of Yb:YAG are superior to those of Yb:YGG and Yb:GGG. The larger emission cross section-lifetime product ($\sigma\tau$) will lead to lower laser thresholds and the lower pump saturation irradiance will reduce pump brightness requirements, assuming similar absorption lengths for the different materials. Guided-mode geometries are well known for their effective enhancement of pump irradiance length products [16], and the pump saturation irradiances for all of these materials are significantly below what can be readily achieved using low-cost, low-brightness, diode-bar-based pump sources coupled to a guided-wave geometry.

Table 1. Optical properties of the PLD grown Yb garnets

Material	Yb:YAG	Yb:YGG	Yb:GGG
Upper state lifetime (μs)	950	985	1270
Emission cross section near 1030 nm (cm^2)	2.0×10^{-20}	0.90×10^{-20}	0.92×10^{-20}
$\sigma\tau$ ($\text{cm}^2 \cdot \text{ms}$)	1.9×10^{-20}	0.89×10^{-20}	1.2×10^{-20}
Absorption cross section near 940 nm (cm^2)	0.8×10^{-20}	0.5×10^{-20}	0.5×10^{-20}
Pump saturation irradiance near 940 nm ($\text{kW} \cdot \text{cm}^{-2}$)	28	43	33

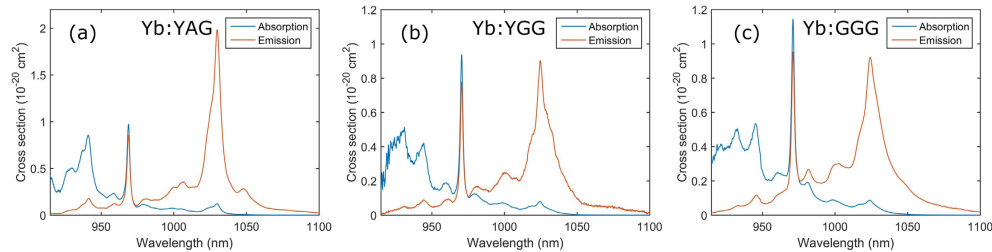


Fig. 1. Absorption and emission cross sections for the garnets. (a) Yb:YAG, (b) Yb:YGG, and (c) Yb:GGG.

4. Diode-pumped laser experiments

The waveguides were mounted on a 5-axis translation stage (3 spatial dimensions, roll and yaw). A pump input mirror was placed close to one waveguide end facet, with the Fresnel reflection from the garnet-air interface at the other waveguide end facet acting as an output coupler and providing a nominal reflectivity of 8.3%. Light from a fast and slow-axis-collimated, conduction-cooled, 940 nm diode bar was focused such that the fast-axis focus was 10.6 μm in diameter at the entrance facet of the waveguide. In the slow axis a 1.5 mm diameter beam waist was formed midway along the waveguide. This arrangement provides close to confocal pumping for the diode's slow axis in the unguided axis of the planar waveguide and for 40 W of launched power, pump irradiance of $>200 \text{ kW/cm}^2$ is achieved (more than $7 \times$ the pump saturation irradiance and $>100 \times$ the pump irradiance required to reach transparency for Yb:YAG). The laser output was collected using an aspheric lens and reflected by a dichroic mirror onto a power meter. Another power meter was placed behind the dichroic mirror to measure unabsorbed pump light, with the estimated absorbed power taken as the difference between pump power transmitted through the pump input mirror and the pump power transmitted through the final dichroic mirror. The experimental setup is shown in Fig. 2. Laser oscillation was achieved for each of the three garnets and the performance is illustrated in Fig. 3. It should be noted that the Yb:YAG performance is the result of extensive optimization of the growth conditions for the film, while the YGG and

GGG films have not received the same level of optimization at this stage and further improvements in performance are likely to result from further growth optimization.

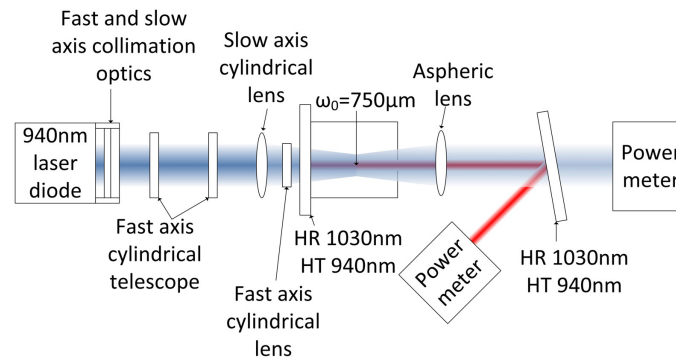


Fig. 2. Experimental configuration for the diode pumped waveguide laser experiments.

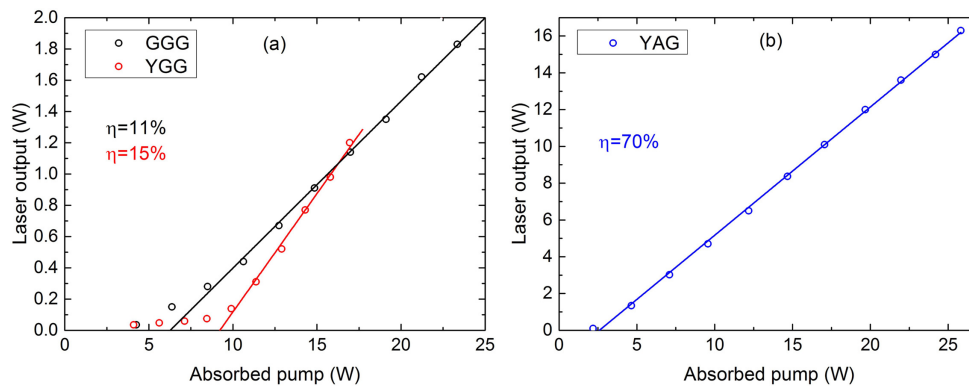


Fig. 3. Laser performance of the diode pumped waveguide lasers. (a) Yb:GGG and YGG, and (b) Yb:YAG.

5. High-brightness pumping

The performance of the diode-bar-pumped Yb:YAG planar waveguide laser warranted investigation of this film under diffraction-limited pumping. A 946 nm Nd:YAG laser with an $M^2 < 1.1$ was used as a pump source; this had the two orthogonal transverse axes of the beam focused to diameter of $10 \mu\text{m}$ to couple into the guided axis of the waveguide, and quasi-collimated at $100 \mu\text{m}$ diameter through the unguided axis. This diameter of $100 \mu\text{m}$ was selected to be smaller than the cavity mode size for a plane-plane cavity stabilized by a moderate thermal lens, therefore favoring the fundamental resonator mode over higher-order resonator modes and leading to a diffraction-limited output. For this experiment the pump input mirror was affixed to the pump input facet of the waveguide with a fluorinated liquid and the other end of the guide was left open, again relying on the Fresnel reflection to provide feedback. Identical slope efficiencies are achieved to those obtained with the previous diode-bar pumping and a laser threshold of 150 mW is observed, see Fig. 4. The beam quality for this Yb:YAG waveguide laser was close to diffraction-limited in both axes, with a measured M^2 of 1.25 for the guided axis and 1.15 for the unguided axis at the maximum output power of 260 mW . This beam quality confirms the absence of any significant scattering centers within the waveguide and evidences the suitability of this technique for the fabrication of waveguides producing diffraction-limited output at high average power - either by relying on

external stable cavities or monolithic unstable resonators. When running at full power with 530 mW of absorbed pump, the resonator mode was 210 μm in diameter in the unguided axis. This corresponds to a plane-plane cavity with an effective thermal lens of focal length $f \sim 250$ mm.

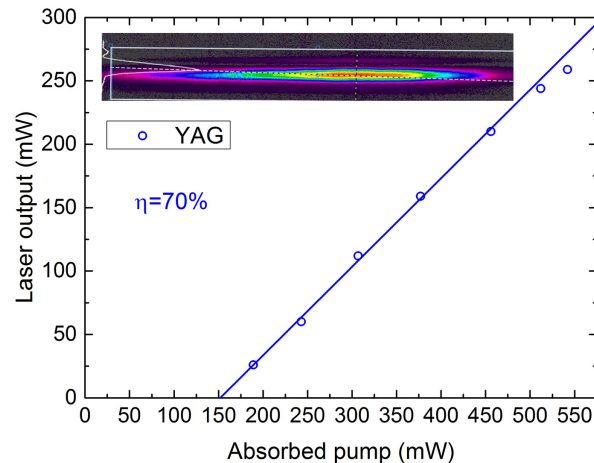


Fig. 4. Laser performance of the 946 nm pumped Yb:YAG waveguide laser with inset of the laser mode. The roll-off in efficiency at higher pump powers is likely to be due to evaporation of the fluorinated liquid used to adhere the pump input mirror. Inset, image of laser mode at full output power of 260 mW. The laser mode diameter is 210 $\mu\text{m} \times 10 \mu\text{m}$.

6. Conclusions

We have demonstrated Watt-level output from lasers built around three different PLD-grown Yb-doped garnet crystals. The performance of our PLD-grown Yb:YAG is now close to that of Czochralski-grown Yb:YAG, which we believe is the first report of a PLD-grown laser crystal achieving this. The initial performance of Yb:YGG and Yb:GGG is promising and these materials, grown onto YAG substrates, allow high index contrast and therefore the potential to move to double-clad structures; as has previously been demonstrated with Yb:Y₂O₃ [17].

Funding

Engineering and Physical Sciences Research Council (EPSRC) (EP/L021390/1 and EP/N018281/1). The work undertaken as part of this funding, as per Research Data Management policy, can be found at DOI: 10.5258/SOTON/403961.